

# Diagnostic accuracy of MRI with extracellular vs. hepatobiliary contrast material for detection of residual hepatocellular carcinoma after locoregional treatment

Jordi Rimola <sup>1,2</sup> Matthew S. Davenport,<sup>2</sup> Peter S. Liu,<sup>2,3</sup> Theodore Brown,<sup>4</sup> Jorge A. Marrero,<sup>5,6</sup> Barbara J. McKenna,<sup>4</sup> and Hero K. Hussain<sup>2</sup>

<sup>1</sup>BCLC Group, Radiology Department, Hospital Clínic Barcelona, University of Barcelona, Villarroel 170 Escala 3 Planta 1, 08036 Barcelona, Catalonia, Spain

<sup>2</sup>Department of Radiology, University of Michigan Health System, Ann Arbor, MI, USA

<sup>3</sup>Abdominal Imaging Institute, Cleveland Clinic, Cleveland, OH, USA

<sup>4</sup>Department of Pathology, University of Michigan Health System, Ann Arbor, MI, USA

<sup>5</sup>Department of Hepatology, University of Michigan Health System, Ann Arbor, MI, USA

<sup>6</sup>Division of Digestive and Liver Diseases, Department of Internal Medicine, University of Texas Southwestern Medical Center, Dallas, TX, USA

## Abstract

**Purpose:** To compare the diagnostic accuracy of extracellular gadolinium-based contrast-enhanced MRI (Gd-MRI) and gadoxetic acid-enhanced MRI (EOB-MRI) for the assessment of hepatocellular carcinoma (HCC) response to locoregional therapy (LRT) using explant correlation as the reference standard.

**Methods:** Forty-nine subjects with cirrhosis and HCC treated with LRT who underwent liver MRI using either Gd-MRI ( $n = 26$ ) or EOB-MRI ( $n = 23$ ) within 90 days of liver transplantation were included. Four radiologists reviewed the MR images blinded to histology to determine the size and percentage of viable residual HCC using a per-lesion explant reference standard. Sensitivities, specificities, accuracies, and agreement with histology for the detection residual HCC were calculated.

**Results:** Gd-MRI had greater agreement with histology (ICC: 0.98 [0.95–0.99] vs. 0.80 [0.63–0.90]) and greater sensitivity for viable HCC (76% [13/17 50–93%] vs. 58% [7/12; 28–85%]) than EOB-MRI; specificities were similar (84% [16/19; 60–97%] vs. 85% [23/27; 66–96%]). Areas under ROC curves for detecting residual viable tumor

were 0.80 (0.64–0.92) for Gd-MRI and 0.72 (0.55–0.85) for EOB-MRI. Gd-MRI had greater inter-rater agreement than EOB-MRI for determining the size of residual viable HCC (ICC: 0.96 [0.92–0.98] vs. 0.85 [0.72–0.92]). **Conclusion:** Gd-MRI may be more accurate and precise than EOB-MRI for the assessment of viable HCC following LRT.

**Key words:** Hepatocellular carcinoma—Liver—Magnetic resonance imaging—Radiofrequency ablation—Trans-arterial chemoembolization

## Abbreviations

HCC	Hepatocellular carcinoma
MR	Magnetic resonance
Gd-MRI	Gadolinium-based contrast-enhanced MRI
EOB-MRI	Gadoxetic acid-enhanced MRI
LRT	Locoregional treatment
ROC	Receiver operator characteristics
RFA	Radiofrequency ablation
TACE	Trans-arterial chemoembolization
EASL	European Association for the Study of the Liver

**Electronic supplementary material** The online version of this article (<https://doi.org/10.1007/s00261-018-1775-x>) contains supplementary material, which is available to authorized users.

Correspondence to: Jordi Rimola; email: [jrimola@clinic.cat](mailto:jrimola@clinic.cat)

Assessment of response to locoregional therapy (LRT) is essential in the management of hepatocellular carcinoma

(HCC) [1, 2]. Objective response to radiofrequency ablation (RFA) and trans-arterial chemoembolization (TACE) has been shown to improve overall and progression-free survival in randomized controlled trials and cohort studies [1, 3–8], and may be associated with lower rates of HCC recurrence after liver transplantation [9]. Lack of objective response after one or more therapies may portend poor survival, although this is controversial and influenced by the type of therapy used [10–14]. Currently, MRI plays a pivotal role in the evaluation of therapeutic response after LRT. When HCC is incompletely treated after LRT, residual or recurrent tumors typically manifest as focal or multifocal nodular arterial-phase hyperenhancement. The relationship between post-LRT nodular arterial-phase hyperenhancement and viable HCC was initially proposed at the Barcelona conference of the European Association for the Study of the Liver (EASL) in 2000 [15], and has been further endorsed by other international societies [16–19].

Although it is clear that liver MRI adds value in the management of patients with HCC undergoing LRT, it is less certain whether this imaging is best performed with a nonspecific extracellular contrast agent (Gd-MRI) or a hepatobiliary imaging agent such as gadoxetate disodium (EOB-MRI). Some studies have reported that EOB-MRI has a high sensitivity for the diagnosis of HCC, including those  $\leq 2$  cm, and that EOB-MRI is more sensitive than multiphase contrast-enhanced computed tomography for detecting HCC  $\leq 1$  cm [20–23]. Moreover, some international guidelines and initiatives have suggested specific diagnostic criteria for HCC based on findings with EOB-MRI [24–27], and some authors have advocated use of EOB-MRI in the assessment of LRT treatment response [25].

However, there is a lack of comparative data between Gd-MRI and EOB-MRI in this setting, and Watanabe et al. [28] have suggested that use of an hepatobiliary imaging agent is either not helpful or degrades diagnostic accuracy. Although the hepatobiliary phase may improve detection of small foci of HCC in the non-treated liver, it may be less effective following LRT, in which zones of benign liver show decreased or absent contrast material uptake due to devitalization or hepatocyte injury. In post-LRT imaging, the arterial phase becomes especially important, and the arterial phase with EOB-MRI is on average weaker than that of Gd-MRI due to poorer enhancement at recommended dosing and an increased propensity for motion-related artifacts [29, 30]. The trade-off with EOB-MRI between the disadvantages of the arterial phase and the advantages of the hepatobiliary phase raise the question of which contrast agent type is ideal when imaging patients with HCC following LRT. The purpose of our study was to compare the diagnostic accuracy of Gd-MRI and EOB-MRI for the assessment of HCC response to LRT using explant correlation as the reference standard.

## Methods

Institutional review board approval was obtained and informed consent waived for this HIPAA-compliant single-institution retrospective cohort study.

### *Patient selection*

All subjects undergoing liver transplantation at the study institution between 1/1/2005 and 4/30/2012 ( $n = 544$ ) were reviewed by a single experienced abdominal radiologist with expertise in HCC imaging. Inclusion criteria for the study population were: (a) HCC identified on MRI prior to LRT and diagnosed by biopsy or radiological criteria [17, 31] prior to orthotopic liver transplantation (OLT), (b) The HCC was treated with LRT prior to OLT, and (c) Post-LRT Gd-MRI or EOB-MRI performed within 90 days prior to OLT. Subjects who underwent liver transplantation without an a priori diagnosis of HCC and/or no contrast-enhanced liver MRI prior to transplantation ( $n = 466$ ), or those who had HCC that was not treated with LRT before OLT ( $n = 29$ ), were not included (Fig. 1). The final study population included 49 subjects with HCC managed with LRT prior to OLT who underwent pre-operative Gd-MRI ( $n = 26$  [17 male, 9 female]) or EOB-MRI ( $n = 23$  [17 male, 6 female]) within 90 days of OLT.

### *MRI acquisition protocol*

MRI examinations were performed on either a 1.5T (Achieva XR, Philips Healthcare; LX Signa Excite 2, GE Healthcare) or 3.0T (Ingenia, Philips Healthcare) magnet on the basis of magnet availability. Magnet strength was allocated based on availability—neither was clinically preferred over the other. Pulse sequence details are provided in Table 1. Pre- and dynamic post-contrast imaging were obtained using an axial T1-weighted three-dimensional spoiled gradient-recalled-echo sequence with selective fat suppression performed during suspended respiration. Arterial-phase timing was based on manual fluoroscopic (Achieva XR, Philips Healthcare; Ingenia, Philips Healthcare) or automated contrast material bolus tracking (SmartPrep; GE Healthcare). Dynamic post-contrast timing was: arterial (20–30 s), venous (60–90 s), late dynamic or transitional (120–150 s), delayed (180–210 s; Gd-MRI only), and hepatobiliary (20 min; EOB-MRI only).

The dose of extracellular gadolinium (either gadobenate dimeglumine [MultiHance; Bracco Diagnostics, Princeton NJ] or gadopentetate dimeglumine [Magnevist; Bayer Healthcare; Wane NJ]) was according to patient weight (0.1 mmol/kg; maximum dose, 20 mL) and was power-injected intravenously at a rate of 2 mL/sec followed by a 20-mL saline chaser (2 mL/sec). The dose of gadoxetate disodium (Eovist; Bayer Healthcare,

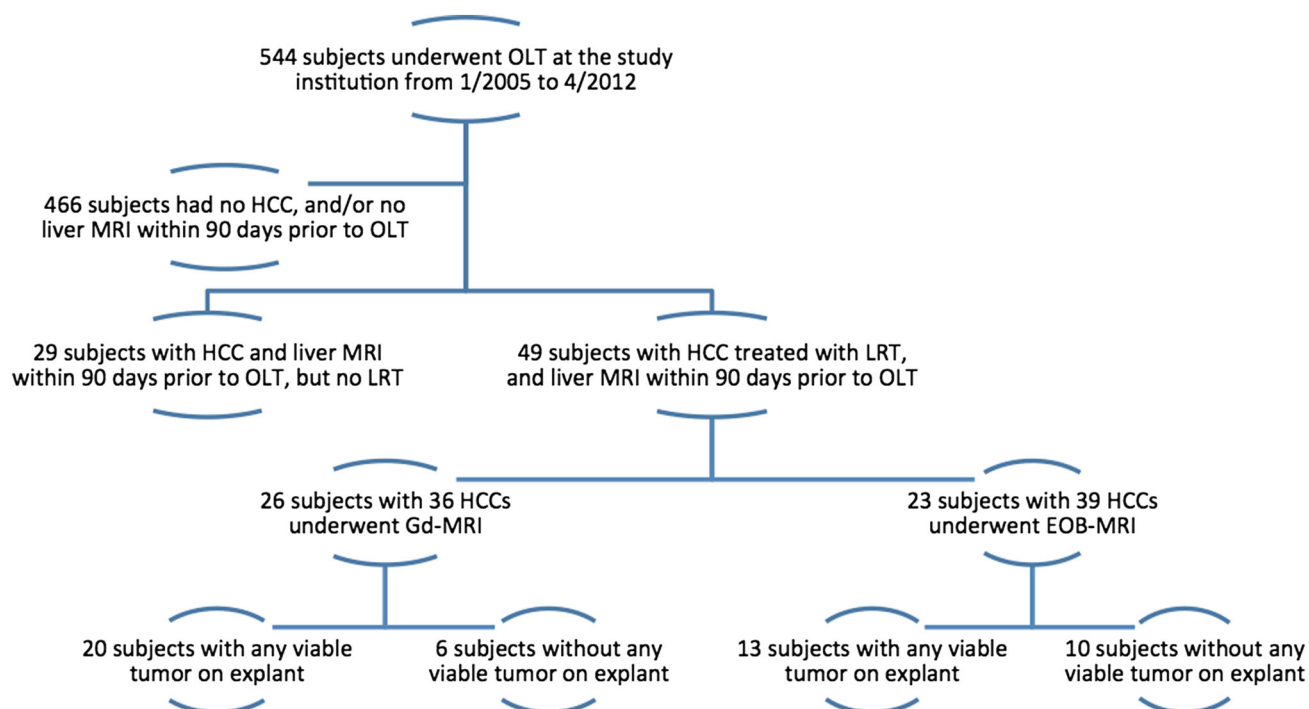


Fig. 1. Study population flow diagram. *OLT* orthotopic liver transplant, *Gd-MRI* MRI with an extracellular agent, *EOB-MRI* MRI with gadoxetate disodium.

Table 1. Liver MRI technical parameters

Sequence	Plane	TR/TE (msec)	Flip angle	Thickness/gap (mm)	FOV
Breath-hold single-shot T2w	Coronal	shortest/255	90°	8/0	Abdomen
Breath-hold single-shot TSE	Axial	shortest/235	90°	8/0	Liver
Breath-hold T1w dual-echo GRE	Axial	185/2.3, 4.6	70°	8/0	Liver
Respiratory-triggered FS T2w FSE	Axial	shortest/90	90°	8/0	Liver
DWI (0 and 800 s/mm <sup>2</sup> )	Axial	–	–	6/0	Liver
3D T1w FS SPGR (dynamic)	Axial	3.6/1.3	12°	4/0	Liver
3D T1w FS SPGR (hepatobiliary) <sup>a</sup>	Axial	3.6/1.3	12°/30°	4/0	Liver

*TR* repetition time, *TE* echo time, *T2w* T2-weighted, *TSE* turbo spin echo, *FS* fat-saturated, *FSE* fast spin echo, *T1w* T1-weighted, *SPGR* spoiled gradient-recalled echo, *DWI* diffusion-weighted imaging

<sup>a</sup>Gadoxetate disodium-enhanced MRI only

Wayne, NJ) was fixed at 10 mL diluted with 10 mL saline, and was power-injected intravenously at a rate of 2 mL/sec followed by a 20-mL saline chaser (2 mL/sec).

### Image interpretation

All patient identifiers were removed from each MR examination and the images were networked to a picture archiving and communications workstation (Horizon Medical Imaging PACS; McKesson, Richmond, Canada) under a dummy identifier. The examinations available for review for each subject included the *index* MRI performed immediately prior to OLT, and the *reference* MRI performed immediately prior to the first LRT. Subjects were determined to be in the Gd-MRI cohort if their index MRI was performed with an extracellular

gadolinium-containing contrast agent and in the EOB-MRI cohort if their index MRI was performed with gadoxetate disodium.

Imaging review was performed by four board-certified abdominal fellowship-trained radiologists who were blinded to the explant results and who staff the institutional liver tumor board at their accredited transplant center. To enable a per-lesion assessment with the reference standard, each HCC to be evaluated by the reviewers was identified on a spread sheet by sequence number, image number, and hepatic segment. The review was conducted in two ways. First, two of the four radiologists, with 7 and 5 years of experience in interpreting liver MRI, independently reviewed the index and reference MRI examinations and recorded the following data for each HCC on the index MRI: (a) maximum diameter

of the treated HCC (mm) including all viable and non-viable components, (b) presence of viable HCC using EASL criteria (binary outcome) [15, 16], (c) maximum diameter of any viable HCC (mm), and (d) estimated percentage (0–100%) of viable HCC relative to the reference MRI tumor maximum diameter. Next, the remaining two radiologists with 15 and 10 years of experience in interpreting liver MR images reviewed in consensus the index and reference MRI examinations and recorded the same data. The consensus review was done with the results from the first two readers available for review but blinded to the pathology results. All imaging sequences were available for review for all reference and index MRI examinations.

The independent imaging review was done to establish inter-rater agreement and to determine the range of agreement between imaging and histology. The consensus review was done to determine the maximum performance of each contrast agent and to minimize the effects of inter-rater disagreement.

### Reference standard

The reference standard was one-to-one per-lesion explant histology following OLT. An explant reference standard was chosen because it is the most accurate method of determining the size and volume of residual viable HCC. Histology review was conducted retrospectively by two board-certified pathologists in consensus who were aware of the location of each HCC in the study group but were otherwise blinded to the imaging results.

Explants were evaluated by pathology to measure the greatest diameter of tumors. Representative sections of tumors were submitted for histology, stained with hematoxylin and eosin, and reviewed to estimate the percentage of viable and necrotic areas of each tumor. In addition, the morphology and greatest radial diameter of viable tumor were documented. HCCs distant from the target HCCs in the study population were not part of the analysis.

### Statistical analysis

Continuous data are expressed as means or medians depending on normality; normal data were compared using Student's *t* test. Categorical data are expressed as counts and percentages and compared with  $\chi^2$  test. Diagnostic accuracy was assessed with sensitivity, specificity, accuracy (true positive plus true negative divided by all cases), area under the receiver operating characteristic (ROC) curve, positive predictive value, and negative predictive value. Inter-rater agreement and imaging-histology agreement were expressed with intraclass correlation coefficients (ICC). ICC results were interpreted as follows: < 0.00 (poor), 0.00–0.20 (slight), 0.21–0.40 (fair), 0.41–0.60 (moderate), 0.61–0.80 (sub-

stantial), and 0.81–1.00 (almost perfect) [32]. The primary outcome measure was detection of any viable HCC on the index MRI during the consensus imaging review. Secondary outcome measures included: detection of minimum viable HCC of 5 mm, 10 mm, 5% volume, and 10% volume on index MRI; inter-rater agreement for percent viable HCC and viable HCC diameter; and imaging-histology agreement for percent viable HCC. A *p* value < 0.05 was considered statistically significant. 95% confidence intervals were calculated. Calculations were performed with MedCalc Version 16.2.1.

## Results

The details of the study population are provided in Table 2. There was no significant difference in patient sex (*p* = 0.8), patient age (*p* = 0.3), cause of cirrhosis (*p* = 0.6), pre-LRT HCC tumor burden (*p* = 0.3), or type of LRT used (*p* = 0.6) between the Gd-MRI and EOB-MRI study groups. Forty-six examinations were acquired on 1.5T whereas the remaining 3 examinations were acquired on 3.0T magnet. A total of 36 HCCs were assessed by Gd-MRI (17 after RFA and 19 after TACE) and 39 HCC were assessed by EOB-MRI (19 after RFA, 18 after TACE, 1 after stereotactic body radiotherapy [SBRT], and 1 after combined RFA first and afterwards, TACE). There was no significant difference between contrast agent groups in the number of treated HCCs (*p* = 0.2) or in the largest treated HCC (*p* = 0.3). All of

**Table 2.** Details of the extracellular gadolinium-enhanced MRI (Gd-MRI) and gadoxetate disodium-enhanced MRI (EOB-MRI) study populations

	Gd-MRI	EOB-MRI	<i>p</i>
Sex			0.8
Male	17	17	
Female	9	6	
Age (mean, range)	57 (54–59)	57 (55–59)	0.3
Cause of cirrhosis			0.6
Hepatitis C	18	15	
Hepatitis B	2	1	
Alcohol	2	1	
Cryptogenic	1	4	
Other <sup>a</sup>	3	2	
Pre-treatment HCC burden			
Number of HCCs (median, IQR)	1.0 (1.0–1.4)	1.0 (1.0–2.0)	0.2
Largest HCC (mm, median, IQR)	24 (19–38)	33 (25–36)	0.3
Locoregional therapy			0.6
Radiofrequency ablation	12	11	
Trans-arterial chemoembolization	14	10	
Other <sup>b</sup>	–	2	

Data in parentheses are ranges or interquartile ranges (IQR)

<sup>a</sup>Non-alcoholic steatohepatitis (*n* = 2), alpha-1 antitrypsin deficiency (*n* = 1), primary biliary cirrhosis (*n* = 1), primary sclerosing cholangitis (*n* = 1)

<sup>b</sup>Stereotactic body radiation therapy (*n* = 1), combined RFA and TACE (*n* = 1)

**Table 3.** Inter-rater and rater-histology agreement for viable HCC size (maximum diameter), and percentage of viable HCC referent to the pre-treatment tumor maximum diameter (i.e., % viable), using a per-lesion explant reference standard

	Reader 1 vs. reader 2	Reader 1 vs. histology	Reader 2 vs. histology	Consensus vs. histology
<b>Gd-MRI</b>				
Viable HCC size				
All HCCs	0.96 (0.92–0.98)	–	–	–
RFA-treated HCCs	0.94 (0.83–0.97)	–	–	–
TACE-treated HCCs	0.94 (0.85–0.97)	–	–	–
% Viable HCC				
All HCCs	0.93 (0.87–0.96)	0.88 (0.77–0.94)	0.95 (0.91–0.98)	0.97 (0.95–0.98)
RFA-treated HCCs	0.98 (0.94–0.99)	0.95 (0.88–0.98)	0.93 (0.80–0.97)	0.95 (0.88–0.98)
TACE-treated HCCs	0.89 (0.72–0.95)	0.82 (0.52–0.93)	0.98 (0.94–0.99)	0.98 (0.96–0.99)
<b>EOB-MRI</b>				
Viable HCC size				
All HCCs	0.85 (0.72–0.92)	–	–	–
RFA-treated HCCs	0.92 (0.80–0.97)	–	–	–
TACE-treated HCCs	0.51 (0.26–0.81)	–	–	–
% Viable HCC				
All HCCs	0.98 (0.97–0.99)	0.80 (0.62–0.89)	0.80 (0.62–0.89)	0.80 (0.62–0.89)
RFA-treated HCCs	0.79 (0.43–0.91)	0.73 (0.30–0.89)	0.62 (0.36–0.85)	0.83 (0.54–0.93)
TACE-treated HCCs	0.98 (0.97–0.99)	0.81 (0.50–0.92)	0.83 (0.55–0.92)	0.81 (0.53–0.93)

Results are expressed as inter-class correlation coefficients with 95% confidence intervals for extracellular gadolinium-based contrast-enhanced MRI (Gd-MRI) and gadoxetate disodium-enhanced MRI (EOB-MRI)  
*RFA* radiofrequency ablation, *TACE* trans-arterial chemoembolization

the HCCs in our cohort were hypervascular on the reference MRI (i.e., there were no hypovascular HCCs analyzed).

### *Inter-rater and imaging-histology agreement for assessing response to locoregional therapy*

Inter-rater agreement was almost perfect for both the assessment of viable HCC size and the percentage of viable HCC for Gd-MRI and EOB-MRI [Table 3]. Agreement was significantly greater for Gd-MRI compared to EOB-MRI for the determination of viable HCC size (0.96 [95% CI 0.92–0.98] vs. 0.85 [0.72–0.92]). Both readers independently had greater imaging-histology agreement with Gd-MRI compared to EOB-MRI [Table 3]. The consensus image review demonstrated significantly greater imaging-histology agreement for percentage of viable HCC with Gd-MRI compared to EOB-MRI (ICC: 0.97 [95% CI 0.95–0.98] vs. 0.80 [95% CI 0.62–0.89]).

### *Assessment of complete response to locoregional therapy*

Based on consensus review, Gd-MRI was more sensitive (76% [13/17; 95% CI 50–93%] vs. 58% [7/12; 95% CI 28–85%]) and had a higher positive predictive value (81% [13/16; 95% CI 54–96%] vs. 64% [7/11; 95% CI 31–89%]) than EOB-MRI for the detection of any viable HCC, but these differences were not statistically significant due to wide confidence intervals [Table 4]. Specificity, accuracy, and negative predictive value were similar for Gd-MRI and EOB-MRI (Table 4 and Supplementary Table 1).

The area under the ROC curve for detection of complete response was higher for Gd-MRI compared to EOB-MRI, but this difference was not statistically significant (0.80 [95% CI 0.64–0.92] vs. 0.72 [95% CI 0.55–0.85]).

### *Expanded criteria for determining therapeutic response*

To account for microscopic mismatches between MRI and histology, we conducted a variety of secondary analyses on a sliding scale reference standard for the detection of a minimum amount of viable HCC on explant (5 mm, 10 mm, 5%, and 10%) (Supplementary Table 2). Gd-MRI outperformed EOB-MRI for most thresholds, but these differences were not statistically significant [Supplementary Table 2].

## **Discussion**

Accurate assessment of residual viable HCC following LRT is necessary to determine treatment efficacy, to triage patients to appropriate management, and to predict patient outcome [1,15,27–33]. Early data for EOB-MRI reporting high sensitivity for the diagnosis of small (< 2 cm) HCCs has raised the possibility that EOB-MRI may be equivalent to or superior to Gd-MRI for post-LRT imaging [34]. However, EOB-MRI has limitations with the arterial phase [35], and most studies investigating EOB-MRI focus on its diagnostic accuracy in the pre-treatment liver. Therefore, there is a need to directly compare EOB-MRI to Gd-MRI in the post-LRT setting.

In our series, we found that Gd-MRI showed higher accuracy than EOB-MRI for the detection of viable HCC following LRT (ICC 0.98 vs. 0.80), and higher sensitivity than EOB-MRI for the detection of residual viable HCC (76% vs. 58%) while specificities of both contrast agents were similar (84% vs. 85%). Also, Gd-MRI displayed greater inter-rater agreement than EOB-MRI when determining the size of residual viable HCC (ICC 0.96 vs. 0.85). In combination, our results suggest that Gd-MRI may be more accurate and precise than EOB-MRI for the assessment of viable HCC following LRT. Although a larger cohort and a direct comparison are necessary to validate these findings, we hypothesize that our results indicate that in this context the benefits of the hepatobiliary phase are not outweighed by the limitations of the arterial phase (Fig. 2) [35–37].

Using a sliding scale of reference standards, we explored whether there was a threshold effect in the assessment of LRT efficacy relative to the volume of viable HCC. We assumed that microscopic or otherwise minimal residual tumor diagnosed on explant histology may be misdiagnosed by MRI as complete response, while the clinical impact and need of retreatment at this point remains unclear. However, changing the threshold of the reference standard had little impact on the mea-

**Fig. 2.** **A–E** A 2.5 cm treatment zone in segments 5/6 after radiofrequency ablation on **A** pre contrast, **B** arterial-phase, **C** portal-venous phase, and **D** hepatobiliary (HB) phase images, and **E** the HCC before treatment. The treatment zone is hyperintense in signal relative to liver parenchyma on pre contrast T1-weighted fat suppressed GRE imaging (arrow in **A**), due to coagulation necrosis. No apparent hyperenhancement is seen within or around the area of coagulation necrosis neither on arterial-phase imaging (**B**) nor on portal-venous phase (**C**), or decreased uptake in the HB phase (**D**) relative to the original HCC (arrow in **E**). The appearance suggests complete response to therapy with no residual HCC. At pathology, the treatment zone was 80% necrotic with 20% residual HCC at the periphery.

sured diagnostic accuracy for either type of contrast medium.

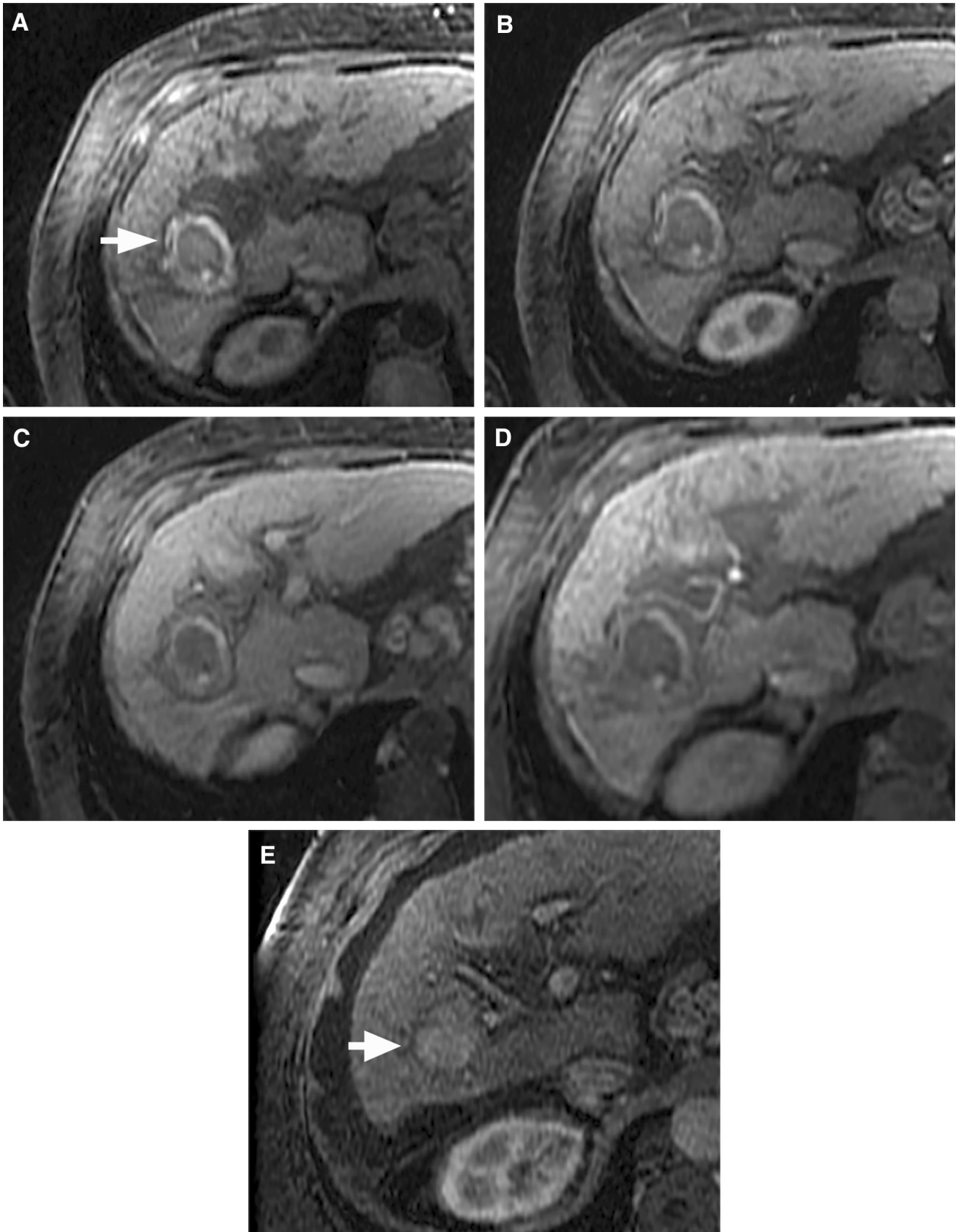
When compared to other studies that have investigated the diagnostic accuracy of Gd-MRI for the detection of complete necrosis following LRT using EASL criteria, our results for Gd-MRI were similar [19, 38, 39]. In those studies, the sensitivity of Gd-MRI was 69–77% and the specificity of Gd-MRI was 91–92%, compared to 76% sensitivity and 84% specificity in the current work [38, 39]. Overall, these data reflect the inherent limitation of Gd-MRI to detect small foci of

**Table 4.** Diagnostic accuracy following blinded consensus expert review of extracellular gadolinium-based contrast-enhanced MRI (Gd-MRI) and gadoxetate disodium-enhanced MRI (EOB-MRI) for the detection of any residual viable hepatocellular carcinoma following locoregional therapy using a per-lesion explant reference standard

	Gd-MRI	EOB-MRI
Prevalence of viable HCC		
All HCCs <sup>a</sup>	47% (17/36)	31% (12/39)
RFA-treated HCCs	41% (7/17)	21% (4/19)
TACE-treated HCCs	53% (10/19)	37% (7/19)
Sensitivity		
All HCCs <sup>a</sup>	76% (13/17; 50–93%)	58% (7/12; 28–85%)
RFA-treated HCCs	71% (5/7; 29–96%)	25% (1/4; 6–80%)
TACE-treated HCCs	80% (8/10; 44–97%)	57% (4/7; 18–90%)
Specificity		
All HCCs <sup>a</sup>	84% (16/19; 60–97%)	85% (23/27; 66–96%)
RFA-treated HCCs	70% (7/10; 35–93%)	87% (13/15; 60–98%)
TACE-treated HCCs	89% (8/9; 52–99%)	83% (10/12; 52–98%)
Accuracy		
All HCCs <sup>a</sup>	81% (29/36; 68–94%)	77% (30/39; 64–90%)
RFA-treated HCCs	71% (12/17; 49–92%)	73% (14/19; 54–93%)
TACE-treated HCCs	84% (16/19; 60–97%)	73% (14/19; 54–93%)
Positive predictive value		
All HCCs <sup>a</sup>	81% (13/16; 54–96%)	64% (7/11; 31–89%)
RFA-treated HCCs	62% (5/8; 25–91%)	33% (1/3; 8–90%)
TACE-treated HCCs	89% (8/9; 52–99%)	67% (4/6; 22–97%)
Negative predictive value		
All HCCs <sup>a</sup>	80% (16/20; 56–94%)	82% (23/28; 63–94%)
RFA-treated HCCs	78% (7/9; 40–97%)	81% (13/16; 54–96%)
TACE-treated HCCs	80% (8/10; 44–97%)	77% (10/13; 46–94%)
Area under ROC curve		
All HCCs <sup>a</sup>	0.80 (0.64–0.92)	0.72 (0.55–0.85)
RFA-treated HCCs	0.71 (0.44–0.89)	0.56 (0.31–0.78)
TACE-treated HCCs	0.84 (0.60–0.97)	0.70 (0.45–0.88)

Ranges in parentheses are 95% confidence intervals

<sup>a</sup>1 HCC evaluated by EOB-MRI was treated by stereotactic body radiotherapy (SBRT)



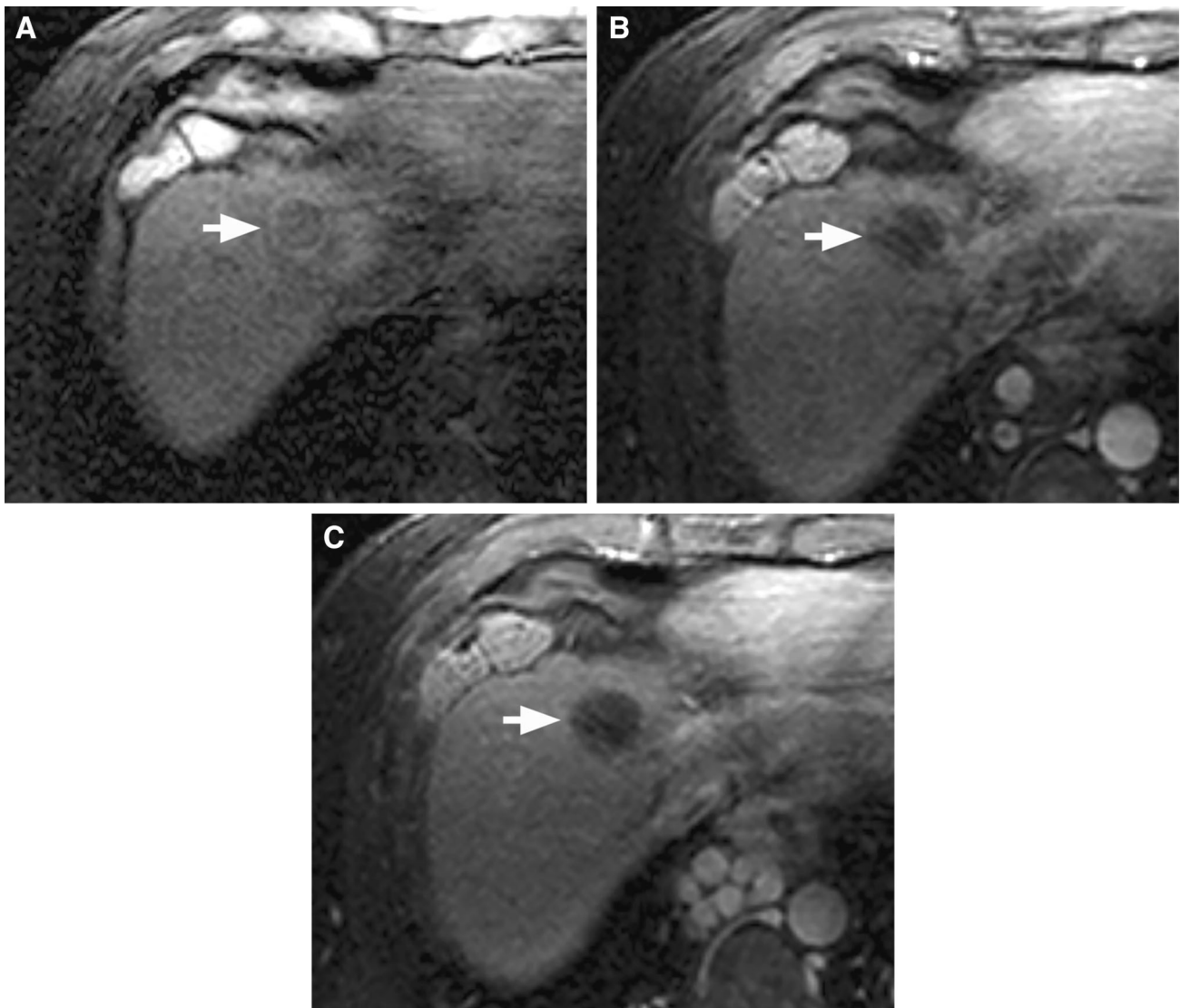


**Fig. 3. A–C** A 3 cm treatment zone in segment 4 (arrows) after radiofrequency ablation on **A** pre-contrast, **B** arterial-phase, and **C** venous phase images. The treatment zone is hypointense in signal relative to liver parenchyma with hyperintense rim on pre contrast T1-weighted fat suppressed gradient-recalled-echo (GRE) imaging (**A**). No

apparent hyperenhancement is seen within or around the area of necrosis on arterial-phase imaging (**B**) or washout appearance in the venous phase (**C**). The appearance suggests complete response to therapy with no residual HCC. At pathology, the treatment zone was 90% necrotic with 10% residual HCC at the periphery.

residual viable HCC after LRT (Fig. 3). This may be caused by a variety of factors, including: (a) limited spatial resolution of MRI, (b) confounding from treatment-related enhancement, or (c) hypoperfusion of treated yet viable HCC.

To our knowledge, only one previous study has evaluated the diagnostic accuracy of EOB-MRI after HCC ablation [28]. In that study, the diagnostic accuracy for locally recurrent HCC was not improved by including the hepatobiliary phase, and hepatobiliary-phase hypointensity could not distinguish reactive therapeutic responses from persistent or recurrent tumor. Although our study did not attempt to determine the contribution

of each phase in the diagnosis of viable HCC, our results also suggest that the hepatobiliary phase has a small effect in the evaluation of LRT efficacy. This is in contradistinction to the effect of the hepatobiliary phase in the non-treated liver, in which the hepatobiliary phase has been shown to improve reader confidence [40].

Our study is subject to the limitations of a retrospective analysis. It was conducted over a 7.3-year period and therefore the image quality may have changed over that time. However, the EOB-MRI examinations were only performed after 2008, and therefore any technical bias based on examination timing would have favored EOB-MRI. Our results reflect an indirect comparison

between both contrast agents using different cohorts of patients. Although both cohorts have similar characteristics, it is possible that undetected selection bias may exist. Explant review was restricted to the slides that were sectioned at the time of clinical evaluation. It is possible that some of the HCCs would have been sectioned differently had this study been part of a prospective trial. The current diagnostic criteria of viable active HCC were based on detection of arterial enhancing areas on the treated HCC and the contribution of specific sequences, such as hepatobiliary or diffusion-weighted imaging [41, 42], was not explicitly assessed as its contribution as diagnostic criteria has not been validated [19], but all sequences were available for review during image interpretation. Our study population did not include any hypovascular HCCs. Therefore, our results only pertain to the post-treatment evaluation of typical hypervascular HCCs. Finally, because of the challenges in obtaining an explant reference standard for patients who have undergone LRT for HCC, the number of subjects included is relatively small ( $n = 49$  subjects with 75 HCCs) and therefore the confidence intervals on our estimates are relatively wide. A larger series would be needed to improve the precision of our estimates.

In conclusion, Gd-MRI may be more accurate and precise than EOB-MRI for the assessment of viable HCC following LRT. The primary benefits of Gd-MRI over EOB-MRI appear to be improved sensitivity with maintained specificity, a more accurate determination of the proportion of viable tumor, and a superior agreement across readers. Future research with a larger cohort also taking advantage of an explant reference standard will be necessary to validate these findings.

#### Compliance with ethical standards

**Funding** Jordi Rimola was partially supported by a grant from Fundació Alfonso Martín Escudero.

**Conflict of interest** The authors of this manuscript declare no relationships with any companies, whose products or services may be related to the subject matter of the article.

**Ethical approval** Institutional Review Board approval was obtained. Written informed consent was waived by the Institutional Review Board. This article does not contain any studies with animals performed by any of the authors.

#### References

- Llovet JM, Di Bisceglie AM, Bruix J, et al. (2008) Design and endpoints of clinical trials in hepatocellular carcinoma. *J Natl Cancer Inst* 100:698–711
- Lewandowski RJ, Mulcahy MF, Kulik LM, et al. (2010) Chemoembolization for hepatocellular carcinoma: analysis in a 172-patient cohort. *Radiology* 255:955–965
- Llovet JM, Real MI, Montaña X, et al. (2002) Arterial embolisation or chemoembolisation versus symptomatic treatment in patients with unresectable hepatocellular carcinoma: a randomised controlled trial. *Lancet* 359:1734–1739
- Lo C-M, Ngan H, Tso W-K, et al. (2002) Randomized controlled trial of transarterial lipiodol chemoembolization for unresectable hepatocellular carcinoma. *Hepatology*. 35:1164–1171
- Llovet JM, Bruix J (2003) Systematic review of randomized trials for unresectable hepatocellular carcinoma: chemoembolization improves survival. *Hepatology*. 37:429–442
- Llovet JM, Ricci S, Mazzaferro V, et al. (2008) Sorafenib in advanced hepatocellular carcinoma. *N Engl J Med*. 359:378–390
- Dhanasekaran R, Khanna V, Kooby DA, et al. (2010) The effectiveness of locoregional therapies versus supportive care in maintaining survival within the Milan criteria in patients with hepatocellular carcinoma. *J Vasc Interv Radiol* 21:1197–1204
- Memon K, Kulik L, Lewandowski RJ, et al. (2011) Radiographic response to locoregional therapy in hepatocellular carcinoma predicts patient survival times. *Gastroenterology* 141:526–535
- Lao OB, Weissman J, Perkins JD (2009) Pre-transplant therapy for hepatocellular carcinoma is associated with a lower recurrence after liver transplantation. *Clin Transplant* 23:874–881
- Sala M, Llovet JM, Vilana R, et al. (2004) Initial response to percutaneous ablation predicts survival in patients with hepatocellular carcinoma. *Hepatology* 40:1352–1360
- Gillmore R, Stuart S, Kirkwood A, et al. (2011) EASL and mRECIST responses are independent prognostic factors for survival in hepatocellular cancer patients treated with transarterial embolization. *J Hepatol* 55:1309–1316
- Georgiades C, Geschwind J-F, Harrison N, et al. (2012) Lack of response after initial chemoembolization for hepatocellular carcinoma: does it predict failure of subsequent treatment? *Radiology* 265:115–123
- Prajapati HJ, Spivey JR, Hanish SI, et al. (2013) mRECIST and EASL responses at early time point by contrast-enhanced dynamic MRI predict survival in patients with unresectable hepatocellular carcinoma (HCC) treated by doxorubicin drug-eluting beads transarterial chemoembolization (DEB TACE). *Ann Oncol* 24:965–973
- Reig M, Rimola J, Torres F, et al. (2013) Postprogression survival of patients with advanced hepatocellular carcinoma: rationale for second-line trial design. *Hepatology* 58:2023–2031
- Bruix J, Sherman M, Llovet JM, et al. (2001) Clinical management of hepatocellular carcinoma. Conclusions of the Barcelona-2000 EASL conference. European Association for the Study of the Liver. *J Hepatol* 35:421–430
- Dufour JF, Greten TF, Raymond E, et al. (2012) Clinical practice guidelines EASL—EORTC clinical practice guidelines: management of hepatocellular carcinoma European Organisation for Research and Treatment of Cancer. *J Hepatol* 56:908–943
- Bruix J, Sherman M (2011) Management of hepatocellular carcinoma: an update. *Hepatology* 53:1020–1022
- Marrero JA, Kulik LM, Sirlin CB, et al. (2018) Diagnosis, staging and management of hepatocellular carcinoma: 2018 Practice Guidance by the American Association for the Study of Liver Diseases. *Hepatology*. <https://doi.org/10.1002/hep.29913>
- Galle PR, Forner A, Llovet JM, et al. (2018) EASL clinical practice guidelines: management of hepatocellular carcinoma. *J Hepatol*. <https://doi.org/10.1016/j.jhep.2018.03.019>
- Ahn SS, Kim M-J, Lim JS, et al. (2010) Added value of gadoxetic acid—enhanced hepatobiliary phase MR imaging in the diagnosis of hepatocellular carcinoma. *Radiology* 255:459–466
- Di Martino M, Marin D, Guerrisi A, et al. (2010) Intraindividual comparison of gadoxetate disodium-enhanced MR imaging and 64-section multidetector CT in the detection of hepatocellular carcinoma in patients with cirrhosis. *Radiology* 256:806–816
- Seong HK, Kim SH, Lee J, et al. (2009) Gadoxetic acid-enhanced MRI versus triple-phase MDCT for the preoperative detection of hepatocellular carcinoma. *Am J Roentgenol* 192:1675–1681
- Roberts LR, Sirlin CB, Zaiem F, et al. (2018) Imaging for the diagnosis of hepatocellular carcinoma: a systematic review and meta-analysis. *Hepatology* 67:401–421
- Kudo M, Matsui O, Izumi N, et al. (2014) Surveillance and diagnostic algorithm for hepatocellular carcinoma proposed by the liver cancer study group of Japan: 2014 update. *Oncology* 87(Suppl 1):7–21. <https://doi.org/10.1159/000368141>
- Merkle EM, Zech CJ, Bartolozzi C, et al. (2016) Consensus report from the 7th International Forum for liver magnetic resonance imaging. *Eur Radiol* 26:674–682

26. Neri E, Bali MA, Ba-Ssalamah A, Boraschi P, Brancatelli G (2016) ESGAR consensus statement on liver MR imaging and clinical use of liver-specific contrast agents. *Eur Radiol* 26:921–931
27. Mitchell DG, Bruix J, Sherman M, Sirlin CB (2015) LI-RADS (liver imaging reporting and data system): summary, discussion, and consensus of the LI-RADS management Working Group and future directions. *Hepatology* 61:1056–1065
28. Watanabe H, Kanematsu M, Goshima S, et al. (2012) Is gadoxetate disodium-enhanced MRI useful for detecting local recurrence of hepatocellular carcinoma after radiofrequency ablation therapy? *Am J Roentgenol* 198:589–595
29. Davenport MS, Caoili EM, Kaza RK, Hussain HK (2014) Matched within-patient cohort study of transient arterial phase respiratory motion-related artifact in MR imaging of the liver: gadoxetate disodium versus gadobenate dimeglumine. *Radiology* 272:123–131
30. Motosugi U, Bannas P, Bookwalter C, Sano K, Reede S (2016) An investigation of transient severe motion related to gadoteric acid-enhanced MR imaging. *Radiology* 279:93–102
31. Wald C, Russo MW, Heimbach JK, Hussain HK (2013) New OPTN/UNOS policy for liver transplant allocation: standardization of liver imaging, diagnosis, classification, and reporting of hepatocellular carcinoma. *Radiology*. 266:376–382
32. Landis JR, Koch GG (1977) The measurement of observer agreement for categorical data. *Biometrics* 33:159–174
33. Forner A, Ayuso C, Varela M, et al. (2009) Evaluation of tumor response after locoregional therapies in hepatocellular carcinoma. *Cancer* 115:616–623
34. Ferenci P, Fried M, Labrecque D, et al. (2010) Hepatocellular carcinoma (HCC): a global perspective. *J Clin Gastroenterol* 44:239–245
35. Davenport MS, Al-hawary MM, Caoili EM, et al. (2013) Comparison of acute transient dyspnea after intravenous administration of gadoxetate disodium and gadobenate phase image quality 1. *Radiology*. 266:452–461
36. Van Beers BE, Pastor CM, Hussain HK (2012) Primovist, Eovist: what to expect? *J Hepatol* 57:421–429
37. Bashir MR, Castelli P, Davenport MS, et al. (2015) Respiratory motion artifact affecting hepatic arterial phase MR imaging with gadoxetate disodium is more common in patients with a prior episode of arterial phase motion associated with gadoxetate disodium. *Radiology* 274:141–148
38. Kim S, Mannelli L, Hajdu CH, et al. (2010) Hepatocellular carcinoma: assessment of response to transarterial chemoembolization with image subtraction. *J Magn Reson Imaging* 31:348–355
39. Riaz A, Lewandowski RJ, Kulik L, et al. (2010) Radiologic-pathologic correlation of hepatocellular carcinoma treated with chemoembolization. *Cardiovasc Interv Radiol* 33:1143–1152
40. Bashir MR, Gupta RT, Davenport MS, et al. (2013) Hepatocellular carcinoma in a North American population: does hepatobiliary MR imaging with Gd-EOB-DTPA improve sensitivity and confidence for diagnosis? *J Magn Reson Imaging* 40:398–406
41. Mannelli L, Kim S, Hajdu CH, et al. (2009) Assessment of tumor necrosis of hepatocellular carcinoma after chemoembolization: diffusion-weighted and contrast-enhanced MRI with histopathologic correlation of the explanted liver. *AJR Am J Roentgenol* 193:1044–1052
42. Goshima S, Kanematsu M, Kondo H, et al. (2008) Evaluating local hepatocellular carcinoma recurrence post-transcatheter arterial chemoembolization: is diffusion-weighted MRI reliable as an indicator? *J Magn Reson Imaging* 27:834–839